

Light on Dark Matter with Weak Gravitational Lensing

S. Pires, J.-L. Starck and A. Réfrégier

*Laboratoire AIM, CEA/DSM-CNRS-Universite Paris Diderot, IRFU/SEDI-SAP, CEA Saclay,
Orme des Merisiers, 91191 Gif-sur-Yvette, France*

Abstract—This paper reviews statistical methods recently developed to reconstruct and analyze dark matter mass maps from weak lensing observations. The field of weak lensing is motivated by the observations made in the last decades showing that the visible matter represents only about 4-5% of the Universe, the rest being dark. The Universe is now thought to be mostly composed by an invisible, pressureless matter -potentially relic from higher energy theories- called “dark matter” (20-21%) and by an even more mysterious term, described in Einstein equations as a vacuum energy density, called “dark energy” (70%). This “dark” Universe is not well described or even understood, so this point could be the next breakthrough in cosmology.

Weak gravitational lensing is believed to be the most promising tool to understand the nature of dark matter and to constrain the cosmological model used to describe the Universe. Gravitational lensing is the process in which light from distant galaxies is bent by the gravity of intervening mass in the Universe as it travels towards us. This bending causes the image of background galaxies to appear slightly distorted and can be used to extract significant results for cosmology.

Future weak lensing surveys are already planned in order to cover a large fraction of the sky with large accuracy. However this increased accuracy also places greater demands on the methods used to extract the available information. In this paper, we will first describe the important steps of the weak lensing processing to reconstruct the dark matter distribution from shear estimation. Then we will discuss the problem of statistical estimation in order to set constraints on the cosmological model. We review the methods which are currently used especially new methods based on sparsity.

Index Terms—Cosmology : Weak Lensing, Methods : Statistics, Data Analysis

I. INTRODUCTION

According to present observations, we believe that the majority of the Universe is dark, i.e. does not emit electromagnetic radiations. Its presence is inferred indirectly from its gravitational effects: on the motions of astronomical objects and on light propagation.

Weak gravitational lensing has been found to be one of the most promising tools to probe dark matter and dark energy because it provides a method to map directly the distribution of dark matter in the Universe (see [1], [2]). From this dark matter distribution, the nature of dark matter can be better understood and better constraints can be set on dark energy because it affects the evolution of structures. This method is now widely used but, the amplitude of the weak lensing signal is so weak that its detection relies on the accuracy of the techniques used to analyze the data. Each step of the analysis has required the development of advanced techniques dedicated to these applications.

This paper is organized as follow:

Section 2 aims at giving an overview of weak gravitational lensing : the basics of the lensing theory and a brief description of the weak lensing data analysis.

Section 3 will be dedicated to the presentation of the shear estimation problem. It requires the measurement of the shape of millions of galaxies with extremely high accuracy, in the presence of observational problems such as anisotropic Point Spread Function, pixelisation and noise. Methods that are currently used to derive the lensing shear field from the shapes of background galaxies will be described.

Section 4 will address the following inverse problem : how to derive a dark matter mass map from the measured shear field. Because of some observational effects such as noise and complex survey geometry, this problem can be seen as an ill-posed inverse problem. We will present various methods of inversion currently used to reconstruct the dark matter mass map from incomplete shear map especially a recent promising method of interpolation, based on the sparse representation of the data. And we will describe the different filtering methods which are used to reduce the noise in these dark matter mass maps such as linear filters, Bayesian techniques and a recent wavelet method.

Finally, in section 5, we will discuss the problem of statistical information extraction in weak lensing data in order to constrain the cosmological model. We will

introduce different statistics which are of interest in weak lensing data analysis. A recent approach based on sparse representations will be presented.

II. INTRODUCTION TO WEAK LENSING

A. Gravitational Lensing observations

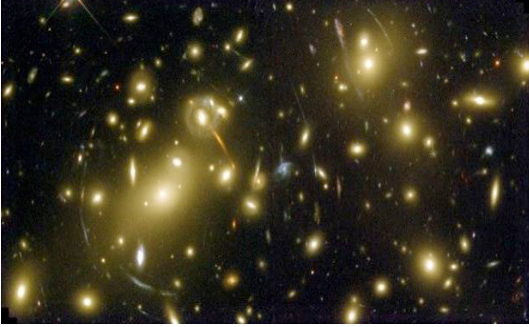


Fig. 1. Strong Gravitational Lensing effect observed in the Abell 2218 cluster (W. Couch et al, 1975 - HST).

In the beginning of the twentieth century, A. Einstein predicted that massive bodies could be seen as gravitational lenses that bend the path of light rays by creating a local curvature in space-time. One of the first confirmations of Einstein's new theory was the observation during the 1919 eclipse of the deflection of light from distant stars by the sun. Since then, a wide range of lensing phenomena have been detected. The gravitational deflection of light generated by mass concentrations along light paths produces magnification, multiplication, and distortion of images. These lensing effects are illustrated by Fig. 1 which shows one of the strongest lens observed : Abell 2218, a massive cluster of galaxies some 2 billion light years away towards the constellation Draco. The observed gravitational arcs are actually the magnified and distorted images of galaxies that are about 10 times more distant than the cluster.

B. Gravitational lensing theory

The properties of the gravitational lensing effect depend on all the projected mass density integrated along the line of sight and on the cosmological angular distances between the observer, the lens and the source (see Fig. 2).

1) *The lens equation:* In the thin lens approximation, we consider that the lensing effect comes from a single matter inhomogeneity located between the source and the observer. The system is then divided into three planes: the source plane, the lens plane and the observer plane.

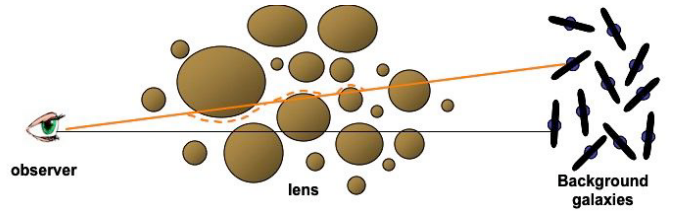


Fig. 2. Illustration of the gravitational lensing effect by large scale structures: the light coming from distant galaxies (on the right) traveling toward the observer (on the left) is bent by the structures (in the middle). This bending causes the image of background galaxies to appear slightly distorted. The structures causing the deformations are called gravitational lenses by analogy with classical optics.

The light ray is supposed to travel without deflection between these planes with just a slight deflection α while crossing the lens plane (see Fig. 3).

In the limit of a thin lens, all the physics of the gravitational lensing effect is contained in the lens equation that relates the true position of the source θ_S to its observed position(s) on the sky θ_I :

$$\vec{\theta}_S = \vec{\theta}_I - \frac{D_{LS}}{D_{OS}} \vec{\alpha}(\vec{\xi}), \quad (1)$$

with $\vec{\xi} = D_{OL}\vec{\theta}_I$ and D_{OL} , D_{LS} and D_{OS} are respectively the distance from the observer to the lens, the lens to the source, and the observer to the source. The deflexion angle α is related to the projected gravitational potential Ψ obtained by the integration of the 3D Newtonian potential $\Phi(\vec{r})$ along the line of sight:

$$\vec{\alpha}(\vec{\xi}) = \frac{2}{c^2} \int \vec{\nabla}_\perp \Phi(\vec{r}) dz = \vec{\nabla}_\perp \underbrace{\left(\frac{2}{c^2} \int \Phi(\vec{r}) dz \right)}_\Psi, \quad (2)$$

where c is the speed of light and $\vec{\nabla}_\perp$ is the perpendicular component of the gradient operator.

We can distinguish two regimes of gravitational lensing. In most cases, the bending of light is small and the background galaxies are just slightly distorted. This corresponds to the weak lensing effect. Sometimes (as seen previously) the bending of light is so extreme, that the light travels along two different paths to the observer, and multiple images of one single source appear on the sky. For this to happen, the lensing effect must be strong. In this paper, we will only address the weak gravitational lensing regime.

2) *The distortion matrix:* The weak gravitational lensing effect results in both an isotropic dilation (the convergence, κ) and an anisotropic distortion (the shear, γ) of the source. To quantify this effect, the lens equation

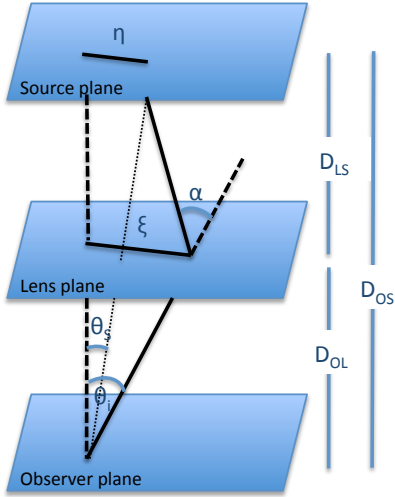


Fig. 3. The thin lens approximation.

has to be solved. Assuming θ_I is small, a first order Taylor series approximation of the distortion operator, given by the lens equation, can be done :

$$\theta_{S,i} = A_{ij}\theta_{I,j}, \quad (3)$$

where i and j correspond respectively to the i^{th} component in the lens plane and the j^{th} component in the source plane and :

$$A_{i,j} = \frac{\partial \theta_{S,i}}{\partial \theta_{I,j}} = \delta_{i,j} - \frac{\partial \alpha_i(\theta_{I,i})}{\partial \theta_{I,j}} = \delta_{i,j} - \frac{\partial^2 \Psi(\theta_{I,i})}{\partial \theta_{I,i} \partial \theta_{I,j}}, \quad (4)$$

where $A_{i,j}$ are the elements of the matrix A and $\delta_{i,j}$ is the Kronecker delta. All the first order effects (the convergence κ and the shear γ) can be described by the Jacobian matrix A that is called distortion matrix:

$$A = (1 - \kappa) \begin{pmatrix} 1 & 0 \\ 0 & 1 \end{pmatrix} - \gamma \begin{pmatrix} \cos 2\varphi & \sin 2\varphi \\ \sin 2\varphi & -\cos 2\varphi \end{pmatrix}, \quad (5)$$

where $\gamma_1 = \gamma \cos 2\varphi$ and $\gamma_2 = \gamma \sin 2\varphi$.

The convergence term κ enlarges the background objects by increasing their size, and the shear term γ stretches them tangentially around the foreground mass.

3) *The gravitational shear (γ):* The gravitational shear γ describes the anisotropic distortions of background galaxy images. It corresponds to a two components field γ_1 and γ_2 that can be derived from the shape of observed galaxies: γ_1 describes the shear in the x and y directions and γ_2 describes the shear in the $x = y$ and $x = -y$ directions. Using the lens equation, the two shear components γ_1 and γ_2 can be related to the

gravitational potential Ψ by:

$$\begin{aligned} \gamma_1 &= \frac{1}{2} \left[\frac{\partial^2 \Psi(\vec{\theta}_I)}{\partial \theta_{I,1}^2} - \frac{\partial^2 \Psi(\vec{\theta}_I)}{\partial \theta_{I,2}^2} \right] \\ \gamma_2 &= \frac{\partial^2 \Psi(\vec{\theta}_I)}{\partial \theta_{I,1} \partial \theta_{I,2}}. \end{aligned} \quad (6)$$

If a galaxy is initially circular with a diameter equal to 1, the gravitational shear will change this galaxy in an ellipsoid with a major axis $a = \frac{1}{1-\kappa-|\gamma|}$ and a minor axis $b = \frac{1}{1-\kappa+|\gamma|}$. The eigenvalues of the amplification matrix (corresponding to the inverse of the distortion matrix A) provide the elongation and the orientation produced on the images of lensed sources [2]. The shear γ is frequently represented by a segment representing the amplitude and the direction of the distortion (see Fig. 4).

4) *The convergence (κ):* The convergence κ that corresponds to the isotropic distortion of background galaxy images is related to the trace of the distortion matrix A by:

$$\begin{aligned} \text{tr}(A) &= \delta_{1,1} + \delta_{2,2} - \frac{\partial^2 \Psi(\vec{\theta}_I)}{\partial \theta_{I,1}^2} - \frac{\partial^2 \Psi(\vec{\theta}_I)}{\partial \theta_{I,2}^2}, \\ \text{tr}(A) &= 2 - \Delta \Psi(\vec{\theta}_I) = 2(1 - \kappa). \end{aligned} \quad (7)$$

The convergence κ is defined as half the Laplacian of the projected gravitational potential $\Delta \Psi$ and is then directly proportional to the projected matter density of the lens (see Fig. 4). For this reason, κ is often considered as the mass distribution.

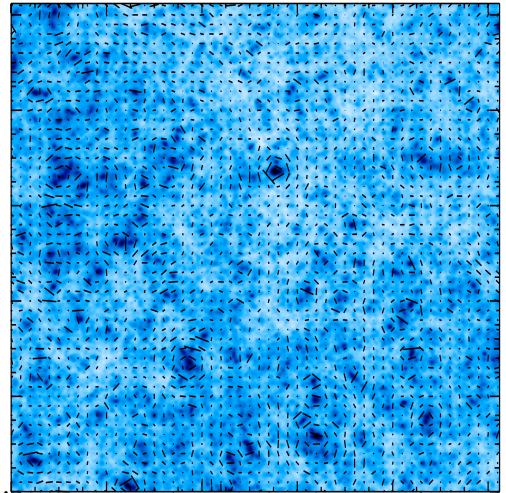


Fig. 4. Simulated convergence map by [3] covering a $2^\circ \times 2^\circ$ field with 1024×1024 pixels. The shear map is superimposed to the convergence map. The size and the direction of the segments represent the amplitude and the direction of the deformation locally.

C. Weak lensing data analysis

The dilation and distortion of images of distant galaxies are directly related to the distribution of the (dark) matter and to the geometry and the dynamics of the Universe. As a consequence, weak gravitational lensing offers unique possibilities for probing the statistical properties of dark matter and dark energy in the Universe. In the next sections, we detail the different steps of the weak lensing data analysis along with the different techniques dedicated to these applications. The following sub-problems will be addressed:

- 1) Shear estimation from the measurement of the background galaxy ellipticities.
- 2) Inversion methods to derive a dark matter mass map from a shear map.
- 3) Filtering of the dark matter mass map to reduce the noise level.
- 4) Statistical analysis of the weak lensing data to constrain the cosmological model.

The constraints that can be obtained on cosmology from the weak lensing effect relies strongly on the quality of the techniques used to analyze the data, because the weak lensing signal is very small. In the following, an overview of the different techniques currently used will be given along with future prospects.

III. SHEAR ESTIMATION

The weak gravitational lensing effect is so small that it is not possible to detect it from a single galaxy. The fundamental problem is that galaxies are not intrinsically circular, so the measured ellipticity is a combination of their intrinsic ellipticity ϵ^{int} and the gravitational lensing shear γ . By assuming that the orientation of intrinsic ellipticities of galaxies are random, any systematic alignment arises from gravitational lensing. To estimate the gravitational shear locally, the measurements of many background galaxies must thus be combined.

From this assumption, to perform an estimation of the shear field, we have to correct each galaxy of the field for the Point Spread Function (PSF) due to instrumental and atmospheric effects that distort the apparent shape of background galaxies. A shape determination algorithm has then to be applied to estimate the gravitational shear from background galaxies.

A. Correction of the PSF and shape measurements

A major challenge for weak lensing is the correction for the PSF. Each background galaxy (S) is convolved by the PSF of the imagery system (H) to produce the image that is seen by the instrument (I^{obs}):

$$I^{obs}(\theta) = S(\theta) * H(\theta). \quad (8)$$

This effect can contaminate a true lensing signal and even for the most modern telescopes, this effect is usually at least of the same order of magnitude as the weak gravitational lensing shear, and is often much larger. Then, we must calibrate the PSF using the images of stars. Indeed, stars present in the field and which correspond to point sources, provide a direct measurement of the PSF, and these can be used to model the variation of the PSF across the field by doing an interpolation between the points where stars appear on the image.

In this section, we briefly review the different methods to correct for instrumental and atmospheric distortions. These methods are broadly distinguished in two classes. The first class of methods subtract the ellipticity of the PSF from that of each galaxy while the second class of methods attempt to deconvolve each galaxy from the PSF.

The most used method is the KSB+ method that belongs to the first category. This method is the result of a series of successive improvements of the original KSB method proposed by Kaiser, Squires & Broadhurst [9]. The core of the method is based on the measurement of the ellipticity of the background galaxies. The weighted ellipticity of an object is defined as:

$$\begin{pmatrix} \epsilon_1 \\ \epsilon_2 \end{pmatrix} = \frac{1}{Q_{1,1} + Q_{2,2}} \begin{pmatrix} Q_{1,1} - Q_{2,2} \\ 2Q_{1,2} \end{pmatrix}, \quad (9)$$

where:

$$Q_{i,j} = \frac{\int d^2\theta W(\theta) I(\theta) \theta_i \theta_j}{\int d^2\theta W(\theta) I(\theta)} \quad (10)$$

are the quadrupole moments weighted by a Gaussian function W of scale length r estimated from the object size, I is the surface brightness of the object and θ is the angular distance from the object center.

The PSF correction is obtained by subtracting the star weighted ellipticity ϵ_i^* from the observed galaxy weighted ellipticity ϵ_i^{obs} . The corrected galaxy ellipticity ϵ_i is given by:

$$\epsilon_i = \epsilon_i^{obs} - P^{sm} (P^{sm*})^{-1} \epsilon_i^*, \quad (11)$$

where $i=1,2$ and P^{sm} and P^{sm*} is the smear susceptibility tensors for the galaxy and star, that can be derived from higher-order moments of the images.

This method has been used by many authors although different interpretations of the method have introduced differences between each implementations. One drawback of the KSB+ method is that for non-Gaussian PSFs, the PSF correction is defined poorly mathematically.

In [11], the authors propose a method to account for realistic PSF better by convolving with an additional kernel to eliminate the anisotropic component of the PSF.

The other class of methods attempt a deconvolution of each galaxy from the PSF. The direct deconvolution (of equation 8) requires an inversion matrix and that becomes an ill-posed inverse problem if the matrix H is singular (i.e. can not be inverted). Some methods have been developed to correct for the PSF without a direct deconvolution. These methods try to reproduce the observed galaxies by modeling each unconvolved background galaxy (the background galaxy as it would be seen without a PSF):

$$I^{mod}(\theta) = S^{mod}(\theta) * H^*(\theta). \quad (12)$$

The modeled galaxy (S^{mod}) is then convolved by the PSF estimated from the stars present in the field (H^*) and the galaxy model is tuned so that the convolved model (I^{mod}) reproduces the observed galaxy (I^{obs}). One major problem of these methods is that a parametric Gaussian shape is assumed for the PSF and depending on the survey the Gaussian functions are sometimes badly suited to represent PSF shapes.

All the methods work by estimating for each galaxy an ellipticity ϵ (after PSF correction) whose definition can vary between the different methods. The accuracy of the shear measurement method depends on the technique used to estimate the ellipticity of the galaxies in presence of observational effects such as noise, poor pixelisation, etc. In the KSB+ method, the ellipticity is derived from quadrupole moments weighted by a Gaussian function. This method has been used by many authors but it is not sufficiently accurate for future surveys. The extension of KSB+ to higher order moments has been done to allow more complex galaxy shapes. Other methods [6], [7], based on the ‘‘shapelet’’ formalism (see [8]) are more accurate but many shapelet coefficients are needed to represent a galaxy. Indeed, the basis functions of shapelets representation constructed from Hermite polynomials weighted by a Gaussian function are not optimal to represent galaxy shapes that are closer to exponential functions. By consequence, in presence of noise, the accuracy of the shear measurement method based on a shapelet decomposition is not optimal.

Many other methods have been developed to address the global problem of the shear estimation. In preparation for the next generation of wide-field survey, a wide range of the shear estimation methods have been compared blindly in the Shear Testing Program (STEP) in order to improve the accuracy of the methods ([4], [5]). Several

methods have achieved an accuracy of a few percents in the simulated STEP images. However, the accuracy required for future surveys will be greater (of the order of 0.1%) and will require new insights. A new challenge called GREAT08 ([10]) has been recently set outside the weak lensing community as an effort to spur further developments.

B. Shear field estimation

After PSF correction, a catalogue of galaxies can be built with the shape and position of each galaxy present in the field. As stated above, the measured shape after PSF correction ϵ is a combination of the intrinsic ellipticity of the galaxy ϵ^{int} and the gravitational lensing shear γ . Thus, the gravitational lensing shear γ can only be estimated by averaging over a large number of galaxies.

Usually this shape catalogue is used to characterize the gravitational shear statistically using correlation functions or other statistics (see section V). It can also be used to map the shear field in order to derive a dark matter mass map (see section IV).

In practice, the shear map is obtained by pixelisation of the field in such a way that several background galaxies fall in each pixel. The shear map is then obtained by averaging for each pixel the ellipticity of the galaxies falling into the pixel:

$$\tilde{\gamma}(i, j) = \frac{1}{N(i, j)} \sum_{k=1}^{N(i, j)} \epsilon(x_k, y_k), \quad (13)$$

where $\tilde{\gamma}$ corresponds to the estimated shear for the pixel (i, j) of the shear map, $N(i, j)$ is the number of galaxies within the pixel (i, j) used to estimate the local shear $\tilde{\gamma}(i, j)$ and $\epsilon(x_k, y_k)$ corresponds to the estimated ellipticity of a galaxy at position (x_k, y_k) . The resulting shear map is subject to some observational effects such as noise that arises both from the measurement error of galaxy ellipticities σ^{meas} and the residual of galaxy intrinsic ellipticities σ^{int} . Another observational effect is the masking out of bright stars from the field that gives a complex geometry to the survey. Fig. 5 shows an example of mask applied to real data. The analysis of weak lensing data requires to account for these observational effects (see section IV-A and section IV-B).

IV. MAPPING THE DARK MATTER

The problem of mass reconstruction has become a central topic in weak lensing since the very first maps of dark matter have demonstrated that we could see the dark side of the Universe.

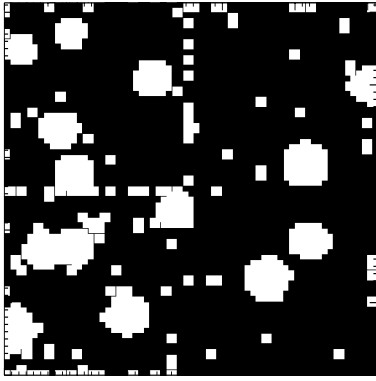


Fig. 5. Mask applied to the CFHTLS data (obtained with the Megacam in the D1 field). The mask covers a field of $1^\circ \times 1^\circ$. (J. Berge et al, 2008)

The reconstruction of the dark matter mass map from shear measurements is an ill-posed inverse problem because of observational effects such as noise, complex geometry of the field, etc. This inverse problem can be decomposed in two sub-problems: the reconstruction of the dark matter mass map from the shear field (section IV-A) and the filtering of the dark matter mass map (section IV-B).

A. Weak lensing inversion

1) *Local inversion*: We first consider the local inversions that have the advantage to address two different problems : the problem of missing data and the finite size of the field. A relation between the gradient of $K = \log(1 - \kappa)$ and combinations of first derivatives of $g = \frac{\gamma}{1-\kappa}$ have been derived by [9] :

$$\frac{-1}{1 - |g|^2} \begin{pmatrix} 1 - g_1 & -g_2 \\ -g_2 & 1 + g_1 \end{pmatrix} \begin{pmatrix} g_{1,1} + g_{2,2} \\ g_{2,1} - g_{1,2} \end{pmatrix} \equiv u \quad (14)$$

This equation can be solved by line integration and there exists an infinite number of local inverse formulae which are exact for ideal data on a finite-size field. But they differ in their sensitivity to observational effects such as noise. The reason why different schemes yield different results can be seen by noting that the vector field u (the right-hand side of equation 14) has a rotational component due to noise because it comes from observational estimates.

In [12], the authors have split the vector field u into a gradient part and a rotational part and they derive the best formula that minimizes the sensitivity to observational effects by convolving the gradient part of the vector field u with a given kernel.

The local inversions reduce the unwanted boundary effects but whatever the formula is used, the

reconstructed field is more noisy than that obtained with a global inversion. Another drawback is that the reconstructed dark matter mass map has still a complex geometry that will make the later analysis more difficult.

2) *Global inversion*: A global relation between κ and γ can be derived, from the relations (6) and (7). Indeed, it has been shown by [13] that the least square estimator $\hat{\kappa}_n$ of the convergence $\hat{\kappa}$ in the Fourier domain is:

$$\hat{\kappa}_n(k_1, k_2) = \hat{P}_1(k_1, k_2)\hat{\gamma}_{1n}(k_1, k_2) + \hat{P}_2(k_1, k_2)\hat{\gamma}_{2n}(k_1, k_2), \quad (15)$$

where the hat symbols denotes Fourier transform and:

$$\hat{P}_1(k_1, k_2) = \frac{k_1^2 - k_2^2}{k_1^2 + k_2^2} \text{ and } \hat{P}_2(k_1, k_2) = \frac{2k_1k_2}{k_1^2 + k_2^2}, \quad (16)$$

with $\hat{P}_1(k_1, k_2) \equiv 0$ when $k_1^2 = k_2^2$, and $\hat{P}_2(k_1, k_2) \equiv 0$ when $k_1 = 0$ or $k_2 = 0$. The most important drawback of this method is that it requires a convolution of shears to be performed over the entire sky. As a result, if the observed shear field has a finite size or a complex geometry, then the method can produce artifacts on the reconstructed convergence distribution near the boundaries of the observed field. A solution that has been proposed by [15] to deal with missing data consists in filling-in judiciously the masked regions by performing an ‘‘inpainting’’ method simultaneously with a global inversion. Inpainting techniques are an extrapolation of the missing information using some priors on the solution. This new method uses a prior of sparsity in the solution introduced by [16]. It assumes that there exists a dictionary Φ (here the Discrete Cosine Transform) where the complete data are sparse and where the incomplete data are less sparse. The weak lensing inpainting problem consists of recovering a complete convergence map κ from the incomplete measured shear field γ_i . The solution is obtained by minimizing:

$$\min_{\kappa} \|\Phi^T \kappa\|_0 \text{ subject to } \sum_i \|\gamma_i - M(P_i * \kappa)\|^2 \leq \sigma, \quad (17)$$

where σ stands for the noise standard deviation and M is the binary mask (i.e. $M_i = 1$ if we have information at pixel i , $M_i = 0$ otherwise). This method enables to reconstruct a complete convergence map κ that can be used to do statistic estimation with a good accuracy (see section V). A comparison with other probes of the matter distribution can also be performed. This comparison is usually done after a filtering of the dark matter map (see section IV-B) whose quality will be improved by the absence of missing data.

B. Weak lensing filtering

The convergence map obtained by inversion of the shear field is very noisy even with a global inversion. The noise comes from the shear measurement errors and the residual intrinsic ellipticities present in the shear maps that propagate during the weak lensing inversion. An efficient filtering is required to compare the dark matter distribution with other probes.

1) Non-Bayesian methods:

- Gaussian filter:

The standard method [13] consists in convolving the noisy convergence map κ with a Gaussian window G with standard deviation σ_G :

$$\kappa_G = G * \kappa_n = G * P_1 * \gamma_{1n} + G * P_2 * \gamma_{2n}. \quad (18)$$

The Gaussian filter is used to suppress the high frequencies of the signal. However, a major problem is that the quality of the result depends strongly on the value of σ_G that controls the level of smoothing.

- Wiener filter:

An alternative to Gaussian filter is the Wiener filter ([17], [18]) obtained by assigning the following weight to each k -mode:

$$w(k) = \frac{|\hat{\kappa}(k)|^2}{|\hat{\kappa}(k)|^2 + |\hat{N}(k)|^2}. \quad (19)$$

In theory, if the noise follows a Gaussian distribution, the Wiener filtering provides the minimum variance estimator. However, it is not the best approach, in particular on small scales where non-linear features deviate significantly from gaussianity. However, Wiener filter leads to reasonable results, generally better than the simple Gaussian filter.

2) Bayesian methods:

- Bayesian filters

Some recent filters are based on the Bayesian theory that considers that some prior information can be used to improve the solution. Bayesian filters search for a solution that maximizes the a posteriori probability using the Bayes' theorem :

$$P(\kappa|\kappa_n) = \frac{P(\kappa_n|\kappa)P(\kappa)}{P(\kappa_n)}, \quad (20)$$

where :

- $P(\kappa_n|\kappa)$ is the likelihood of obtaining the data κ_n given a particular convergence distribution κ .
- $P(\kappa_n)$ is the a priori probability of the data κ_n . This terms, called evidence, is simply a

constant that ensures that the a posteriori probability is correctly normalized.

- $P(\kappa)$ is the a priori probability of the estimated convergence map κ . This term codifies our expectations about the convergence distribution before acquisition of the data κ_n .
- $P(\kappa|\kappa_n)$ is called a posteriori probability.

Searching for a solution that maximizes $P(\kappa|\kappa_n)$ is the same that searching for a solution that minimizes the following quantity (Q) :

$$Q = -\log(P(\kappa|\kappa_n)), \quad (21)$$

$$Q = -\log(P(\kappa_n|\kappa)) - \log(P(\kappa)). \quad (22)$$

If the noise is uncorrelated and follows a Gaussian distribution, the likelihood term $P(\kappa_n|\kappa)$ can be written:

$$P(\kappa_n|\kappa) \propto \exp\left(-\frac{1}{2}\chi^2\right), \quad (23)$$

with :

$$\chi^2 = \sum_{x,y} \frac{(\kappa_n(x,y) - \kappa(x,y))^2}{\sigma_{\kappa_n}^2}. \quad (24)$$

The equation (22) can be expressed as follows:

$$Q = \frac{1}{2}\chi^2 - \log(P(\kappa)) = \frac{1}{2}\chi^2 - \beta H, \quad (25)$$

where β is a constant that can be seen as a parameter of regularization and H represents the prior that is added to the solution.

If we have no expectations about the convergence distribution, the a priori probability $P(\kappa)$ is uniform and the maximum a posteriori is equivalent to the well-known maximum likelihood. This maximum likelihood method has been used by [19], [20] to reconstruct the weak lensing field, but the solution needs to be regularized in some way to prevent overfitting the data. It has been done via the a priori probability of the convergence distribution. The choice of this prior is one of the most critical aspects of the Bayesian analysis. An Entropic prior is frequently used but there exists many definitions of the Entropy (see [21]). One that is currently used is the Maximum Entropy Method (MEM) (see [22], [24]).

Some authors ([19], [23]) have also suggested to reconstruct the gravitational potential Ψ instead of the convergence distribution κ , still using a Bayesian approach. But this is clearly better to reconstruct the mass distribution κ directly because it allows a more straightforward evaluation of the uncertainties in the reconstruction.

- Multiscale Bayesian filters

A multiscale maximum entropy prior has been proposed by [24] which uses the intrinsic correlation functions (ICF) with varying width. The multichannel MEM-ICF method consists in assuming that the visible-space image I is formed by a weighted sum of the visible-space image channels I_j , $I = \sum_{j=1}^{N_c} p_j I_j$ where N_c is the number of channels and I_j is the result of the convolution between a hidden image h_j with a low-pass filter C_j , called ICF (Intrinsic Correlation Function) (i.e. $I_j = C_j * o_j$). In practice, the ICF is a Gaussian. The MEM-ICF constraint is:

$$H_{ICF} = \sum_{j=1}^{N_c} |o_j|^{-m_j} |o_j| \log \left(\frac{|o_j|}{m_j} \right). \quad (26)$$

Another approach, based on the sparse representation of the data, has been used by [25] that consists in replacing the standard Entropy prior by a wavelet based prior. Sparse representations of signals have received a considerable interest in recent year. The problem solved by the sparse representation is to search for the most compact representation of a signal in terms of linear combination of atoms in an overcomplete dictionary.

The entropy is now defined as :

$$H(I) = \sum_{j=1}^{J-1} \sum_{k,l} h(w_{j,k,l}). \quad (27)$$

In this approach, the information content of an image I is viewed as sum of information at different scales w_j . The function h defines the amount of information relative to a given wavelet coefficient. Several functions have been proposed for h .

In [26], the most appropriate entropy for the weak lensing reconstruction problem has been found to be the NOISE-MSE entropy that presents a quadratic behavior for small coefficients and is very close to the l_1 norm (i.e. absolute value of the wavelet coefficient) when the coefficient value is large, which is known to produce good results for the analysis of piecewise smooth images. The proposed filter called MRLens (Multi-Resolution for weak Lensing) has shown to outperform other techniques (Gaussian, Wiener, MEM, MEM-ICF) in the reconstruction of dark matter. It has been used to reconstruct the largest weak lensing survey ever undertaken with the Hubble Space Telescope. The result is shown Fig. 6. This map is the most precise and detailed dark matter mass map, covering a large enough area to see extended filamentary structures.

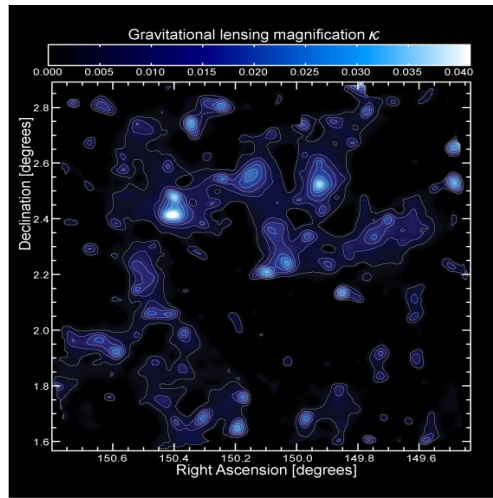


Fig. 6. Map of the dark matter distribution in the 2-square degree COSMOS field by [27]: the linear blue scale shows the convergence field κ , which is proportional to the projected mass along the line of sight. Contours begin at 0.4 % and are spaced by 0.5% in κ .

V. COSMOLOGICAL MODEL CONSTRAINTS

Image distortion measurements of background galaxies caused by large-scale structures provides a direct way to study the statistical properties of the growth of structures in the Universe. Weak gravitational lensing measures the mass and can thus be directly compared to theoretical models of structure formation. But because, we have only one realization of our Universe, a statistical analysis is required to do the comparison. The estimation of the cosmological parameters from weak lensing data can be seen as an inverse problem. The direct problem that consists of deriving weak lensing data from cosmological parameters can be solved using numerical simulations. But the inverse problem cannot be solved so easily because the N-body equations used by the numerical simulations can not be inverted. A statistical analysis is then required to constrain the cosmological parameters. The statistical characteristics of the weak lensing field can be quantified using a variety of measures estimated either in the shear field or in the convergence field. Most lensing studies do the statistical analysis in the shear field to avoid the inversion. But most of the following statistics can also be estimated in the convergence field if the missing data are carefully accounted.

A. Second-order statistics

The most common method for constraining cosmological parameters uses second-order statistics of the shear field calculated either in real or Fourier space (or Spherical Harmonic space).

The most popular Fourier space second-order statistic is the **power spectrum** P_γ because it can be easily

related to the theoretical 3D matter power spectrum $P(k, \chi)$ to estimate cosmological parameters. The correlation properties are more convenient in Fourier space, but for surveys with complicated geometry due to the removal of bright stars, the spatial stationarity is not satisfied and the missing data need proper handling. Consequently, real space statistics are easier to estimate, although statistical error bars are harder to estimate. An example of real space second-order statistic is the **shear variance** $\langle \gamma^2 \rangle$, defined as the variance of the average shear $\bar{\gamma}$ evaluated in circular patches of varying radius θ_s . The shear variance $\langle \gamma^2 \rangle$ can be related to the underlying 3D matter power spectrum via the 2D convergence power spectrum P_γ . This shear variance has been used in many weak lensing analysis to constrain cosmological parameters. Another real space statistic is the **shear two-point correlation function** $\xi_{i,j}(\theta)$ that is currently used because it is easy to implement and can be estimated even for complex geometry. It is defined as follows :

$$\xi_{i,j}(\theta) = \langle \gamma_i(\vec{\theta}^1) \gamma_j(\vec{\theta}^2 + \vec{\theta}) \rangle, \quad (28)$$

where $i, j = 1, 2$ and the averaging is done over pairs of galaxies separated by angle $\theta = |\vec{\theta}|$. By parity $\xi_{1,2} = \xi_{2,1} = 0$ and by isotropy $\xi_{1,1}$ and $\xi_{2,2}$ are functions only of θ . The shear two-point correlation functions can also be related to the underlying 3D matter power spectrum via the 2D convergence power spectrum P_γ . These two-point correlation functions are the most popular statistical tools used in weak lensing analysis. The **variance of the aperture mass** M_{ap} [29] that corresponds to an average shear two-point correlation has been also used in many weak lensing analyses. This statistic is the result of the convolution of the shear two-point correlation with a compensated filter. Several forms of filters have been suggested which trade locality in real space with locality in Fourier space.

Second-order statistics measure the Gaussian properties of the field. This is a limited amount of information since it is known that the low redshift Universe is highly non-Gaussian on small scales. Indeed, gravitational clustering is a non linear process and in particular at small scales the mass distribution is highly non-Gaussian. Consequently, if only second-order statistics are used to set constraints on the cosmological model, degenerate constraints are obtained between some important cosmological parameters.

B. Higher-order statistics

An alternative procedure is to consider higher-order statistics of the weak lensing shear field enabling a

characterization of the non-Gaussian signal.

The **three-point correlation function** $\xi_{i,j,k}$ is the lowest-order statistics which can be used to detect non-Gaussianity.

$$\xi_{i,j,k}(\theta) = \langle \gamma(\vec{\theta}_1) \gamma(\vec{\theta}_2) \gamma(\vec{\theta}_3) \rangle. \quad (29)$$

In Fourier space it is called **bispectrum** and only depends on distances $|\vec{l}_1|$, $|\vec{l}_2|$ and $|\vec{l}_3|$:

$$B(|\vec{l}_1|, |\vec{l}_2|, |\vec{l}_3|) \propto \langle \hat{\gamma}(|\vec{l}_1|) \hat{\gamma}(|\vec{l}_2|) \hat{\gamma}^*(|\vec{l}_3|) \rangle. \quad (30)$$

It has been shown that tighter constraints can be obtained with the three-point correlation function [30].

A simpler quantity than the three-point correlation function is provided by measuring the **third-order moment (skewness)** of the convergence κ that measures the asymmetry of the distribution. The convergence skewness is primarily due to rare and massive dark matter halos. The distribution will be more or less skewed positively depending on the abundance of rare and massive halos. We can also estimate the **fourth-order moment (kurtosis)** of the convergence that measures the peakedness of a distribution. A high kurtosis distribution has a sharper “peak” and flatter “tails”, while a low kurtosis distribution has a more rounded peak.

C. Other non-Gaussian statistics

The weak lensing field is highly non-Gaussian: on small scales, we can observe structures like galaxies, groups and clusters and on larger scales, we observe some filament structures. Another approach to look for non-Gaussianity is to perform a statistical analysis directly on the non-Gaussian structures present in the convergence field. For example, the galaxy clusters that are the largest virialized cosmological structures in the Universe can provide a unique way to focus on non-Gaussianities present at small scales. One interesting statistic is the **peak counting** that searches the number of peaks detected on the convergence field corresponding roughly to the cluster abundance.

D. Statistical approach based on sparsity

It has been proposed by [14] to do a statistical analysis based on the sparse representation of the weak lensing data. Several representations have been compared: Fourier, wavelet, ridgelet and curvelet representations. The comparison shows that the wavelet transform is the most sensitive to non-Gaussian cosmological structures. Indeed, by minimizing the number of large coefficient, the wavelet transform makes statistics be more sensitive to the non-Gaussianities present in the weak lensing field. In the same paper, several non-Gaussian statistics

have been compared and the peak counting estimated in a wavelet representation, called **Wavelet Peak Counting**, has been found to be the best non-Gaussian statistic to constrain cosmological parameters.

VI. CONCLUSION

The weak gravitational lensing effect that is directly sensitive to the gravitational potential provides a unique method to map the dark matter. This can be used to set tighter constraints on cosmological models and to understand better the nature of dark matter and dark energy. But the constraints derived from this weak lensing effect depend on the techniques used to analyze the weak lensing signal which is very weak.

The field of weak gravitational lensing has recently seen great success in mapping the distribution of dark matter (Fig. 6). But new methods are now necessary to reach the accuracy required by future wide-field surveys and ongoing efforts are done to improve the current analyses. This paper attempt to give an overview of the techniques of signal processing that are currently used to analysis the weak lensing signal along with future directions. It shows that the weak lensing is a dynamic research area in constant progress.

In this paper, we have detailed the different steps of the weak lensing data analysis thus presenting various aspects of signal processing. For each problem, we have systematically presented a range of methods currently used from earliest to up-to-date methods. This paper shows that a milestone in weak lensing data analysis progress has been the introduction of Bayesian ideas that have provided a way to incorporate prior knowledge in data analysis. The next one could possibly be the introduction of sparsity. Indeed, we have presented new methods based on sparse representations of the data that have already had some success.

REFERENCES

- [1] M. Bartelmann and P. Schneider, Weak gravitational lensing, Phys. Rept. 340, 291, 2001
- [2] Y. Mellier, Probing the Universe with Weak Lensing, Ann. Rev. Astron. Astrophys. 37, 127, 1999
- [3] C. Vale and M. White, Simulating Weak Lensing by Large-Scale Structure, Astrophysical Journal, 592, 699, 2003
- [4] C. Heymans et al, The Shear Testing Programme 1, Monthly Notices of the Royal Astronomical Society, 368, 1323, 2006
- [5] M. Richard et al, The Shear Testing Programme 2, Monthly Notices of the Royal Astronomical Society, 376, 13, 2007
- [6] G. Bernstein and M. Jarvis, Shapes and Shears, Stars and Smears: Optimal Measurements for Weak Lensing, Astrophysical Journal, 123, 583, 2002
- [7] K. Kuijken, Shears from shapelets, Astronomy and Astrophysics, 456, 827, 2006
- [8] R. Massey and A. Refregier, Polar shapelets, Monthly Notices of the Royal Astronomical Society, 363, 197, 2005
- [9] N. Kaiser, Nonlinear cluster lens reconstruction, Astrophysical Journal Letter, 439, L1, 1995
- [10] S. Bridle et al, Handbook for the GREAT08 Challenge, accepted in Annals of Applied Statistics, 2008
- [11] N. Kaiser, A New Shear Estimator for Weak-Lensing Observations, Astrophysical Journal, 537, 555, 2000
- [12] S. Seitz and P. Schneider, Cluster lens reconstruction using only observed local data: an improved finite-field inversion technique, Astronomy and Astrophysics, 305, 383, 1996
- [13] N. Kaiser and G. Squires, Mapping the dark matter with weak gravitational lensing, Astrophysical Journal, 404, 441, 1993
- [14] S. Pires, J.L. Starck, A. Amara, A. Refregier and R. Teyssier, Cosmological models discrimination with Weak Lensing, submitted to Astronomy and Astrophysics, 2008
- [15] S. Pires, J.L. Starck, A. Amara, R. Teyssier, A. Refregier and J. Fadili, FASTLens (FASt STatistics for weak Lensing) : Fast method for Weak Lensing Statistics and map making, accepted in Monthly Notices of the Royal Astronomical Society, 2009
- [16] M. Elad, J.-L. Starck, P. Querre and D.L. Donoho, Simultaneous cartoon and texture image inpainting using morphological component analysis (MCA), J. on Appl. and Comp. Harm. Anal., 2005
- [17] D.-J. Bacon and A.-N. Taylor, Mapping the 3D dark matter potential with weak shear, Monthly Notices of the Royal Astronomical Society, 344, 1307, 2003
- [18] R. Teyssier, S. Pires, S. Prunet, D. Aubert, C. Pichon, A. Amara, K. Benabed, S. Colombi, A. Refregier and J.-L. Starck, Full-sky weak-lensing simulation with 70 billion particles, Astronomy and Astrophysics, 497, 335, 2009
- [19] M. Bartelmann, R. Narayan, S. Seitz and P. Schneider, Maximum-likelihood Cluster Reconstruction, Astrophysical Journal, 464, L115, 1996
- [20] U. Seljak, Weak Lensing Reconstruction and Power Spectrum Estimation: Minimum Variance Methods, Astrophysical Journal, 506, 64, 1998
- [21] S.-F. Gull, Maximum Entropy and Bayesian Methods, J. Skilling (ed.) Kluwer Academic Publishers, Dordrecht, 53, 1989
- [22] S.-L. Bridle, M. P. Hobson, A. N. Lasenby and R. Saunders, A maximum-entropy method for reconstructing the projected mass distribution of gravitational lenses, Monthly Notices of the Royal Astronomical Society, 299, 895, 1998
- [23] S. Seitz, P. Schneider and M. Bartelmann, Entropy-regularized maximum-likelihood cluster mass reconstruction, Astronomy and Astrophysics, 337, 32, 1998
- [24] P. J. Marshall, M. P. Hobson, S. F. Gull and S. L. Bridle, Maximum-entropy weak lens reconstruction: improved methods and application to data, Monthly Notices of the Royal Astronomical Society, 335, 1037, 2002
- [25] E. Pantin and J.-L. Starck, Deconvolution of astronomical images using the multiscale maximum entropy method, Astronomy and Astrophysics, 118, 575, 1996
- [26] J.-L. Starck, S. Pires and A. Refregier, Weak lensing mass reconstruction using wavelets, Astronomy and Astrophysics, 451, 1139, 2006
- [27] R. Massey et al, Dark matter maps reveal cosmic scaffolding, Nature, 445, 286, 2007
- [28] H. Hoekstra, H. K. C. Yee and M. D. Gladders, Weak Lensing Study of Galaxy Biasing, Astrophysical Journal, 577, 595, 2002
- [29] P. Schneider, L. van Waerbeke, B. Jain and G. Kruse, A new measure for cosmic shear, Monthly Notices of the Royal Astronomical Society, 296, 873, 1998
- [30] M. Takada and B. Jain, Three-point correlations in weak lensing surveys: model predictions and applications, Monthly Notices of the Royal Astronomical Society, 344, 857, 2003